Probing for Extra Top Yukawa Couplings in Light of $t\bar{t}h(125)$ Observation

Wei-Shu Hou, Masaya Kohda and Tanmoy Modak
Department of Physics, National Taiwan University, Taipei 10617, Taiwan
(Dated: February 19, 2024)

The observation of $t\bar{t}h(125)$ production at the Large Hadron Collider (LHC) is the first direct measurement of the top Yukawa coupling. It opens the window on an extra top Yukawa coupling, ρ_{tt}, from a second Higgs doublet, without a Z_2 symmetry to forbid flavor changing neutral Higgs couplings. We show that $t\bar{t}h$ and Higgs property measurements at the High Luminosity LHC can constrain the $\mathrm{Re}\,\rho_{tt}$–$\mathrm{Im}\,\rho_{tt}$ parameter space that could drive electroweak baryogenesis, but the Γ_h width measurement must be considerably improved beyond current projections.

PACS numbers: 14.65.Ha, 14.80.Cp, 14.80.Ec 11.30.Er

arXiv:1806.06018v2 [hep-ph] 14 Oct 2018

I. INTRODUCTION

The CMS and ATLAS experiments announced [1, 2] recently the observation of $pp \to t\bar{t}h^0$ production at the Large Hadron Collider (LHC), where h^0 is the 125 GeV scalar boson discovered not so long ago. The observed production strengths are consistent with the Standard Model (SM) expectation, and constitute the landmark direct detection of the Higgs boson coupling to the top quark, the top Yukawa coupling λ_t. While indirect evidence have long existed, we now have direct experimental proof that $\lambda_t \simeq 1$, as prescribed by $\lambda_t = \sqrt{2}m_t/v$ in the SM, where v is the vacuum expectation value of the Higgs doublet field.

Let us recap the experimental observations. Using 35.9 fb^{-1} data collected in 2016 at 13 TeV collision energy and covering the $h \to WW^*$, ZZ^*, $\gamma\gamma$, $\tau^+\tau^-$ and $b\bar{b}$ final states, together with Run 1 data taken at 7 and 8 TeV, CMS [1] observes the relative strength

$$\mu_{t\bar{t}h} = 1.26^{+0.31}_{-0.26}, \qquad (\text{Run 2} + \text{Run 1, CMS}) \qquad (1)$$

with respect to SM, amounting to 5.2σ significance. The expected significance for SM is 4.2σ. ATLAS had published earlier [3] a Run 2 result based on 36.1 fb^{-1} collected in 2016 and covering the same Higgs decay final states, finding 4.2σ evidence. As a contribution to the LHCP conference held recently in Bologna, ATLAS updated the $h \to \gamma\gamma$ and $h \to ZZ^* \to 4\ell$ modes to a total of 79.8 fb^{-1} data at 13 TeV. Together with the other 3 modes based on 36.1 fb^{-1}, ATLAS observes [2]

$$\mu_{t\bar{t}h} = 1.32^{+0.28}_{-0.26}, \qquad (\text{Run 2 Update, ATLAS}) \qquad (2)$$

at 5.8σ significance (4.9σ), while combining further with Run 1 data, the significance becomes 6.3σ (5.1σ). We have put the SM expectation in parenthesis.

Thus, both ATLAS and CMS have *observed* $t\bar{t}h$ production. We note that both experiments had earlier hints for $t\bar{t}h$ production with strength stronger than SM, which improve the combined significance quoted above.

Since Yukawa couplings are the source of CP violation (CPV) in SM, with direct measurement of top Yukawa coupling attained, it opens up the question whether there are *additional* Yukawa couplings. As there is nothing against the existence of a second doublet, the two Higgs doublet model (2HDM) is in fact one of the most plausible beyond-SM (BSM) possibilities, where one should "naturally" have a second set of Yukawa couplings. However, due to the perceived curse of flavor changing neutral Higgs (FCNH) couplings, Glashow and Weinberg famously eliminated all such extra couplings by demanding "natural" flavor conservation (NFC) [4]: each type of fermion charge receives mass from *just one* Higgs doublet. This enforces only one Yukawa matrix per fermion mass matrix, and they are therefore simultaneously diagonalized: absence of FCNH. There are two ways to implement the NFC condition for quarks, and 2HDM-II, where u-type and d-type quarks receive mass from separate doublets, has been the most popular, as it arises with supersymmetry.

A decade after the Glashow-Weinberg NFC condition, the emerging quark mass-mixing hierarchy led to the critique [5] that NFC may be overkill. As the top quark is the heaviest fermion, the best probe may be $t \to ch$ [6] for FCNH tch coupling. With the observation of $h(125)$ in 2012, it was stressed [7] that the 2×2 extra Yukawa couplings ρ_{cc}, ρ_{ct}, ρ_{tc}, and ρ_{tt} of the *exotic* doublet should be taken seriously [8], and the issue is experimental: we have to demonstrate their nonexistence, rather than *assume* NFC and throw them away. In this paper we address the importance of the flavor-diagonal ρ_{tt}.

The tth coupling in 2HDM without NFC is

$$\mathcal{L}_{tth} = -\frac{1}{\sqrt{2}}\bar{t}_L(-\lambda_t \sin\gamma + \rho_{tt}\cos\gamma)t_R h + \text{h.c.}, \qquad (3)$$

while the tch coupling is (ρ_{ct} is already constrained by flavor physics to be small [7, 9])

$$\mathcal{L}_{tch} = -\frac{1}{\sqrt{2}}\rho_{tc}\cos\gamma\ \bar{t}_L c_R h, \qquad (4)$$

where $\cos^2\gamma \ll 1$ is the alignment phenomenon observed at the LHC [10], the fact that the observed h boson is rather close [11] to the SM Higgs boson. In 2HDM-II, the mixing angle of the two CP-even scalars, $\cos\gamma$, is usually expressed as $\cos(\alpha - \beta)$, but without the NFC condition, or the Z_2 symmetry to implement it, $\tan\beta$ is unphysical, hence we use the different notation [12].

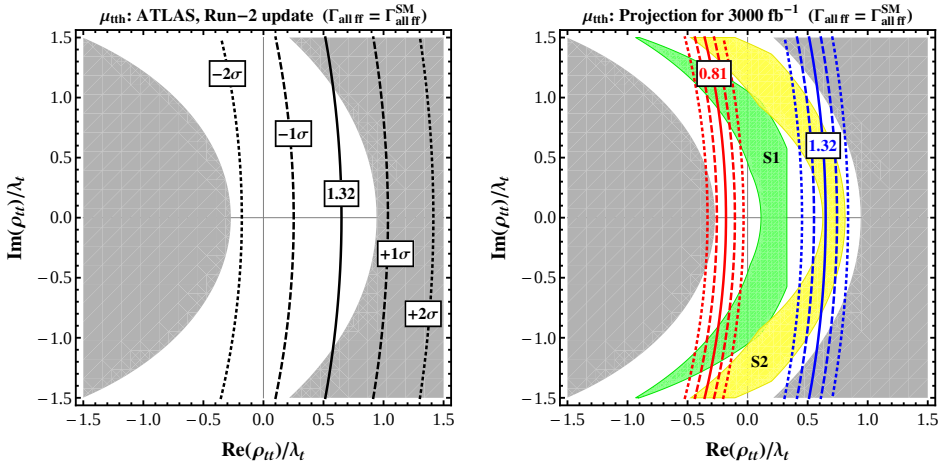


FIG. 1. In both panels, the gray regions represent 2σ exclusion by Run 1 ATLAS-CMS combination [11], while $\mu_{t\bar{t}h}$ (solid) with dashed (dotted) lines for 1σ (2σ) range are for [Left] ATLAS Run-2 update [2]; [Right] projection to full HL-LHC data with central values as marked, allowing 5% and 10% uncertainties. The green (yellow) region in the right panel gives the projected 2σ allowed region in Scenario 1 (2), for full HL-LHC data defined in Eq. (8). We have taken $\cos\gamma = 0.3$ and $\sin\gamma < 0$.

It was recently noted that $\lambda_t \mathrm{Im}\,\rho_{tt}$ can easily drive [13] the baryon asymmetry of our Universe (BAU), or electroweak baryogenesis (EWBG), which needs $\mathcal{O}(1)$ Higgs quartic couplings of the 2HDM for the first order electroweak phase transition. The latter can relatively easily accommodate [12] the observed approximate alignment phenomenon. These add to the attraction of 2HDM without the NFC condition. Note that EWBG is not suppressed by $\cos\gamma$ [13]. Other processes not suppressed by $\cos\gamma$ generally involve the exotic Higgs bosons directly, such as $b \to s\gamma$ [7, 9], $gg \to H^0/A^0 \to t\bar{t}$, $t\bar{c}$ [9], and $cg \to tH^0/tA^0 \to tt\bar{t}$, $tt\bar{c}$, $t\bar{t}c$ [14].

So far, the $t \to ch$ decay has not been observed, with limits approaching 10^{-3} [15]. We assume it is suppressed by ρ_{tc}, but take the maximum $\cos\gamma$ value allowed by data. The point is, even if the admixture of ρ_{tt} into the tth coupling is suppressed by approximate alignment, i.e. $\cos\gamma$, interference with the leading SM λ_t effect provides a sensitive probe in $t\bar{t}h$ production. In the following, we illustrate the new, direct probe of $t\bar{t}h$ production, and compare with indirect probes of $h \to gg$, $\gamma\gamma$ loop processes, projecting into the future of High-Luminosity LHC (HL-LHC). We give a simplified discussion of how other extra Yukawa couplings, such as ρ_{bb}, would affect Γ_h and shift the loop constraint. We offer some remarks on future prospects beyond HL-LHC.

II. INDIRECT AND DIRECT PROBES OF ρ_{tt}

ρ_{tt} and $\cos\gamma$ are constrained by ATLAS and CMS measurements of the Higgs boson production and decay rates. The main effect of ρ_{tt} is for $gg \to h$, which is given by [16, 17]

$$\mu_{gg\mathrm{F}} \equiv \frac{\sigma(gg\to h)}{\sigma(gg\to h)_{\mathrm{SM}}} \simeq \big|(1.05-0.08i)[-\sin\gamma + \cos\gamma\,\mathrm{Re}(\rho_{tt})/\lambda_t] -0.05+0.08i\big|^2 + 2.57[\cos\gamma\,\mathrm{Im}(\rho_{tt})/\lambda_t]^2, \quad (5)$$

through triangle loop diagram, where the absorptive, i.e. explicit i terms arise from light quark loops. The $(\mathrm{Re}\,\rho_{tt})^2$ effect is suppressed by $(\cos\gamma)^2$, or alignment, where we shall take the value of $\cos\gamma = 0.3$ (corresponding to $-\sin\gamma = 0.954$) that may still be allowed by data [9]. Of interest is the $\sin\gamma\cos\gamma$ interference term between the SM and extra Yukawa coupling, which allows better sensitivity to $\mathrm{Re}\,\rho_{tt}$. Although the $(\mathrm{Im}\,\rho_{tt})^2$ term is also suppressed by $(\cos\gamma)^2$, but because the imaginary part of the extra Yukawa coupling leads to a γ_5 coupling, the term receives a numerical factor of order 2.6 (see e.g. Ref. [18] for discussion of pseudoscalar coupling), making $gg \to h$ sensitive to larger values of $(\mathrm{Im}\,\rho_{tt})^2$, which links with EWBG.

The $h \to WW^*$, ZZ^* rates are modified by the overall factor $\sin^2\gamma$ from the SM ones. As for $h \to \gamma\gamma$ decay, which also arises from triangle loop, the rate is only mildly affected [16, 17] by $\cos\gamma\,\rho_{tt}$

$$\mu^{\gamma\gamma} \equiv \frac{\Gamma(h\to\gamma\gamma)}{\Gamma(h\to\gamma\gamma)_{\mathrm{SM}}} \simeq \big|-(1.27+0.01i)\sin\gamma -0.28[-\sin\gamma + \cos\gamma\,\mathrm{Re}(\rho_{tt})/\lambda_t] + 0.01 - 0.01i\big|^2 + 0.18[\cos\gamma\,\mathrm{Im}(\rho_{tt})/\lambda_t]^2, \quad (6)$$

because of W boson dominance in the loop.

Using the Run 1 combination of ATLAS and CMS results [11], constraints on real and imaginary parts of ρ_{tt} for $\cos\gamma = 0.3$ with $\sin\gamma < 0$ are shown in Fig. 1. We use the ten-parameter fit to the three decay channels

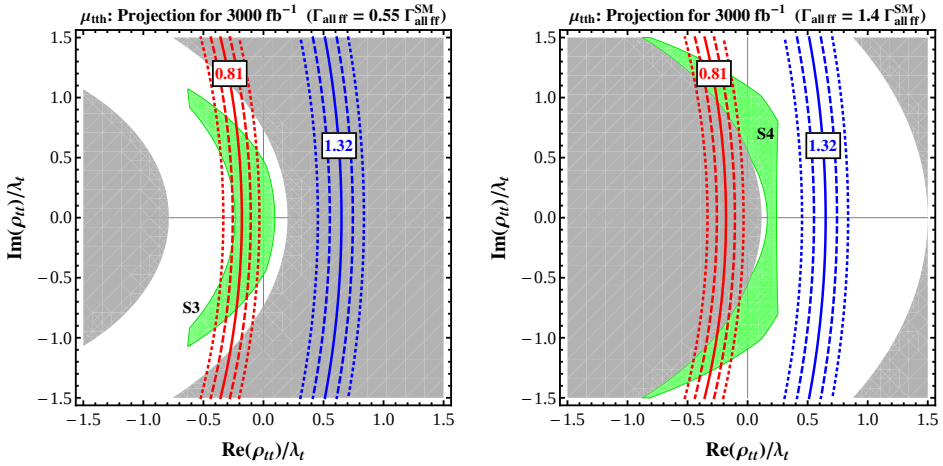


FIG. 2. Same as Fig. 1 [right], but for $\Gamma_{\text{all }ff} = 0.55\Gamma^{\text{SM}}_{\text{all }ff}$ [left], $1.4\Gamma^{\text{SM}}_{\text{all }ff}$ [right]. The green regions are for Scenarios 3 or 4 defined in Eqs. (11) and (12).

$h \to \gamma\gamma, ZZ^*, WW^*$ with ggF+ttH or VBF+VH production, and individual 2σ constraints from the six signal strengths are overlaid, resulting in the gray shaded regions. The right-hand side (r.h.s.) comes from the $h \to WW^*$ decay mode, while l.h.s. comes from $h \to ZZ^*$. The actual sensitivity to $\text{Re}\,\rho_{tt}$ and $\text{Im}\,\rho_{tt}$ is mainly driven by $gg \to h$ production.

For the direct probe of tth coupling, we calculate the $pp \to t\bar{t}h$ cross section at leading order (LO) by Monte Carlo event generator MadGraph5_aMC@NLO [19] with the parton distribution function set NN23LO1 [20]. In particular, we use the Higgs Characterisation model [21] implemented in FeynRules 2.0 [22] framework, where model details can be found in Ref. [23]. We ignored contributions other than from tth coupling. The signal strength for 13 TeV LHC can be approximated by

$$\mu_{t\bar{t}h} \simeq [-\sin\gamma + \cos\gamma\,\text{Re}(\rho_{tt})/\lambda_t]^2 + 0.45[\cos\gamma\,\text{Im}(\rho_{tt})/\lambda_t]^2, \qquad (13\text{ TeV}) \qquad (7)$$

with mild modification of the 0.45 coefficient to 0.46 for 14 TeV LHC. Thus, the $(\text{Re}\,\rho_{tt})^2$ and $(\text{Im}\,\rho_{tt})^2$ terms are suppressed by $|\cos\gamma|^2$, but the $\sin\gamma\cos\gamma$ interference term brings in better sensitivity to $\text{Re}\,\rho_{tt}$. We take the ATLAS Run 2 update of $\mu_{t\bar{t}h}$, Eq. (2), and display the 2σ allowed range in Fig. 1[left] as marked. Because of the mild excess, a positive $\text{Re}\,\rho_{tt}$ is preferred, but partially excluded by the indirect data. However, a broad range of $|\text{Im}\,\rho_{tt}|$ is allowed, extending beyond 1 if the $\text{Re}\,\rho_{tt}$ interference effect is destructive.

Thus, current data between indirect and direct probes of ρ_{tt} are quite consistent with electroweak baryogenesis [13] by 2HDM without NFC.

It is of interest, therefore, to project the reach for HL-LHC. This is shown as the blue and red lines in Fig. 1[right] for $\mu_{t\bar{t}h} = 0.81, 1.32$, corresponding to -2σ and central value in Eq. (2), respectively. Considering the trend in measurements of $\mu_{t\bar{t}h}$, we do not display the $+2\sigma$ case. On the other hand, we take an optimistic 5% as the 1σ uncertainty reach for ultimate HL-LHC sensitivity, based on current projections [24, 25], and anticipating a combination of ATLAS and CMS data.

The signal strength measurements for ggF and VBF production should also improve in the same time frame. With 3000 fb^{-1}, the projected uncertainties by ATLAS and CMS [24, 25] are $\sim 5\%$ for $h \to \gamma\gamma, ZZ^*$ with ggF production, and $\sim 10\%$ for $h \to \gamma\gamma, WW^*$ with VBF production. In Fig. 1[right], HL-LHC projections for these four modes are shown for the two following scenarios:

$$\mu^{\gamma\gamma,ZZ}_{gg\text{F}} = 1,\ \mu^{\gamma\gamma,WW}_{\text{VBF}} = 1 \quad \text{(Scenario 1)},$$
$$\mu^{\gamma\gamma,ZZ}_{gg\text{F}} = 1.2,\ \mu^{\gamma\gamma,WW}_{\text{VBF}} = 0.8 \quad \text{(Scenario 2)}. \qquad (8)$$

Assuming $\pm 10\%$ (20%) ranges for ggF (VBF) modes as 2σ uncertainties with 3000 fb^{-1} data, we overlay the four constraints to obtain the green (denoted as S1) and yellow (S2) allowed regions. We keep the Run 1 exclusion (gray shaded) regions for comparison. In each scenario, the combination of the two ggF modes gives the crescent-shaped allowed region, but $h \to \gamma\gamma$ with VBF production cuts off part of the positive $\text{Re}\,\rho_{tt}$ region in Scenario 1. This is because $\cos\gamma = 0.3$ is a bit too large to sustain SM-like value for $\mu^{\gamma\gamma}_{\text{VBF}}$, which was assumed in Scenario 1. Put differently, if $\cos\gamma$ is not too small, we would have other means (e.g. combined fit) of probing it by the HL-LHC era. We keep $\cos\gamma = 0.3$ for sake of comparison, and to maximize the interference effect.

In Scenario 1, there is no overlap with the $\mu_{t\bar{t}h} \sim 1.32$ band, while overlap with the $\mu_{t\bar{t}h} \sim 0.81$ band implies preference for $|\text{Im}\,\rho_{tt}| \sim 1$. If the latter is found, it would provide insight on EWBG without probing CPV directly. On the other hand, Scenario 2 is compatible with the $\mu_{t\bar{t}h} \sim 1.32$ band, which would imply a nonzero $\text{Re}\,\rho_{tt}$ in the range $0.4 \lesssim \text{Re}\,\rho_{tt} \lesssim 0.8$, with $|\text{Im}\,\rho_{tt}| \lesssim 1.2$.

We have assumed the inclusive results for the $t\bar{t}h$ signal strength. We note that, as data increases, separate production/decay channels would likely be disentangled.

III. SIMPLIFIED EFFECT OF LIGHT FERMIONS

But there is a catch in the discussion above. Analogous to Eq. (3), the 2HDM without NFC brings in extra Yukawa couplings that modify hbb, $h\tau\tau$ and hcc couplings. While they give minor modifications to $gg \to h$ and $h \to \gamma\gamma$, the major impact is on the total h width, Γ_h, which is not well measured yet.

As individual processes are also not yet well measured, rather than several couplings, we treat the partial width of $h \to$ light fermions as the single overall effect,

$$\frac{\Gamma_{\text{all } ff}}{\Gamma^{\rm SM}_{\text{all } ff}} = \frac{\Gamma_{bb} + \Gamma_{\tau\tau} + \Gamma_{cc} + \cdots}{\Gamma^{\rm SM}_{bb} + \Gamma^{\rm SM}_{\tau\tau} + \Gamma^{\rm SM}_{cc} + \cdots}. \tag{9}$$

Taking branching ratio values [26] for $m_h = 125.09$ GeV, the total width is modified as

$$\frac{\Gamma_h}{\Gamma^{\rm SM}_h} \simeq 0.67 \frac{\Gamma_{\text{all } ff}}{\Gamma^{\rm SM}_{\text{all } ff}} + 0.24 \sin^2\gamma + 0.08 \mu_{gg\rm F}. \tag{10}$$

We stress that 2HDM without NFC can relatively easily lead to Γ_h that differs from SM.

Similar to Fig. 1[right], we display the effect of $\Gamma_{\text{all } ff} = 0.55\ (1.4) \Gamma^{\rm SM}_{\text{all } ff}$ in Fig. 2[left] ([right]), where the broad "white crescent" allowed by the Run 1 ATLAS-CMS combination is moved leftward (rightward). For $\Gamma_{\text{all } ff} = 0.55\ \Gamma^{\rm SM}_{\text{all } ff}$, both the ggF and VBF signal strengths tend to be enhanced via the enhancements in the h decay branching ratios. Hence, we tailor the following scenario for the HL-LHC projection:

$$\mu^{\gamma\gamma,ZZ}_{gg\rm F} = 1.2,\ \mu^{\gamma\gamma,WW}_{\rm VBF} = 1.2 \quad \text{(Scenario 3)}, \tag{11}$$

with 2σ range as in Scenarios 1 and 2, shown as the green shaded allowed region in Fig. 2[left]. In this case, the crescent-shaped region is cut from left by $\mu^{\gamma\gamma}_{\rm VBF}$. For $\Gamma_{\text{all } ff} = 1.4\ \Gamma^{\rm SM}_{\text{all } ff}$, the effect for the signal strengths is opposite and, hence, we introduce

$$\mu^{\gamma\gamma,ZZ}_{gg\rm F} = 0.8,\ \mu^{\gamma\gamma,WW}_{\rm VBF} = 0.8 \quad \text{(Scenario 4)}. \tag{12}$$

The 2σ allowed region, shown as the green region in Fig. 2[right], is similar to S1 in Fig. 1[right].

The overlap of the S3 region and $\mu_{t\bar{t}h} \sim 0.81$ band in Fig. 2[left] illustrates the situation where $\text{Re}\,\rho_{tt}$ is slightly negative, with $|\text{Im}\,\rho_{tt}|$ up to 1 fully allowed. The overlap of the S4 region and $\mu_{t\bar{t}h} \sim 0.81$ band in Fig. 2[right] illustrates the situation where $|\text{Im}\,\rho_{tt}| \sim 1$. The $\mu_{t\bar{t}h} \sim 1.32$ band illustrates a tension between indirect and direct probes of ρ_{tt} for both S3 and S4.

What Fig. 2 really illustrates is the need for a better measurement of Γ_h [27]. With current projections at 50% of $\Gamma^{\rm SM}_h$ [28] for HL-LHC, we can only hope that it can be improved with actual data. The 2HDM without NFC would shift all diagonal Yukawa couplings, in principle by same order as the corresponding SM Yukawa coupling, modulated by $\cos\gamma$. More precise measurements of $\mu_{c\bar{c}}$, $\mu_{\tau^+\tau^-}$ and especially $\mu_{b\bar{b}}$ may help. Another approach, for example, is VBF production followed by $h \to VV^*$. Measuring $\mu^{VV^*}_{\rm VBF}$ could probe Γ_h, with only mild dependence on a small $\cos\gamma$.

IV. DISCUSSION AND CONCLUSION

We stress that 2HDM without NFC offer new Yukawa couplings that could alter all ffh couplings from SM values, modulated by $\cos\gamma$. This makes clear the importance of a complete program to measure $\mu_{b\bar{b}}$, $\mu_{\tau^+\tau^-}$, $\mu_{\mu^+\mu^-}$, and even $\mu_{c\bar{c}}$ if charm tagging could be vastly improved.

A second point to note is that each one of these diagonal Yukawa coupling corrections are generally complex. For example, $\text{Im}(\rho_{tt})$ contributes to the electron EDM through two-loop contributions. Under the assumption that the electron Yukawa coupling is SM-like ($\rho_{ee} = 0$) and heavy scalar contributions are negligible, the recent ACME result [29] would imply $|\cos\gamma\,\text{Im}(\rho_{tt})/\lambda_t| < 0.01$ [13, 16]. However, allowing for a complex, in particular imaginary, ρ_{ee} with strength similar to λ_e of SM, it can in principle induce cancellation [13] of the two-loop effect. We had tacitly assumed this in exploring $t\bar{t}h$, and illustrates how the 2HDM without NFC could affect flavor physics. Note that, given that $\lambda_t \cong 1$ is already known, the dominant eigenvalue of the other combination of the two u-type Yukawa matrices, viz. ρ_{tt}, is likely $\mathcal{O}(\lambda_t)$ hence $\mathcal{O}(1)$, and with phase arbitrary. Similar argument would hold for ρ_{bb} and $\rho_{\tau\tau}$.

In contrast to usual effective Lagrangian discussions, the interaction terms reflected in Eqs. (3) and (4) are *as fundamental as* the Yukawa couplings in SM. On one hand, they are well hidden by approximate alignment, or the smallness of $\cos\gamma$. Thus, the direct $pp \to t\bar{t}h$ and other indirect probes would rapidly weaken for smaller $\cos\gamma$. Furthermore, as outlined in Ref. [12], the mass-mixing hierarchy, or some flavor-organization principle, could control FCNH involving lighter generations, and together with approximate alignment, can fully replace the NFC condition to explain the absence of low energy FCNH effects. But alignment need not [12] imply decoupling, and the exotic Higgs sector could well be sub-TeV in mass. If alignment is effective, one would have to probe this exotic Higgs sector, for example via $cg \to tH^0$, tA^0 production, leading to novel $tt\bar{c}$ (same-sign top) and $tt\bar{t}$ (triple top) signatures [14] at the LHC.

With the hope that alignment does not work too well, i.e. $\cos\gamma$ is not overly small, what is the future outlook? First, $\cos\gamma$ should be studied more generally, free of the Z_2 symmetry mindset (i.e. beyond Ref. [10]). A measurement of, rather than constraint on, $\cos\gamma$ would be astounding. Second, improved projections for HL-LHC is expected with a CERN Yellow Report that is under preparation for the European Particle Physics Strategy Update. But the projections must be continuously updated as experience is gained with larger datasets, includ-

ing on Γ_h measurement. Third, we are at the juncture of ILC(250) [30] or CLIC(380) [31] decision. Although these machines are still far away, they provide great hope for much more precision in Higgs property measurements, which would provide better indirect constraints, including on $\delta\Gamma_h$. However, $t\bar{t}h$ production would require at least 500 GeV e^+e^- collision energy.

Thus, the high energy extension of LHC looks more promising for the nearer future on direct $t\bar{t}h$ probe. There is no doubt that a 100 TeV machine [32], though much farther away, would advance the $t\bar{t}h$ and exotic Higgs frontiers by great stride. If the alignment phenomenon reflects [12] $\mathcal{O}(1)$ Higgs quartic couplings within 2HDM, there is likely another layer of BSM physics at the 10 TeV scale to be explored. Finally, we have advocated simple probes of just measuring rates. More sophisticated angular or asymmetry analyses [33] can probe the CPV nature of the tth coupling directly.

In conclusion, the observation of $pp \to t\bar{t}h^0$ at LHC is the first direct measurement of the top Yukawa coupling, and offers a window on the extra Yukawa coupling ρ_{tt} from a second Higgs doublet where the NFC condition is not imposed. The large $\lambda_t \cong 1$ of SM provides the lever arm to probe $\cos\gamma\,\rho_{tt}$ through interference, where $\cos\gamma$ is the CP-even Higgs mixing angle. The parameter space for electroweak baryogenesis offered by this 2HDM can be probed by CP-conserving $t\bar{t}h^0$ production rate and Higgs property measurements. The Achilles heel for this program at the HL-LHC is the knowledge of the h^0 width, Γ_{h^0}, and ATLAS and CMS should put a premium on its improved measurement.

Acknowledgments We thank K.-F. Chen and S. Paganis for discussions. This research is supported by grants MOST 104-2112-M-002-017-MY3, 107-2811-M-002-039, and 106-2811-M-002-187.

[1] A.M. Sirunyan *et al.* [CMS Collaboration], Phys. Rev. Lett. **120**, 231801 (2018).
[2] M. Aaboud *et al.* [ATLAS Collaboration], Phys. Lett. B **784**, 173 (2018).
[3] M. Aaboud *et al.* [ATLAS Collaboration], Phys. Rev. D **97**, 072003 (2018).
[4] S.L. Glashow, S. Weinberg, Phys. Rev. D **15**, 1958 (1977).
[5] T.-P. Cheng, M. Sher, Phys. Rev. D **35**, 3484 (1987).
[6] W.-S. Hou, Phys. Lett. B **296**, 179 (1992).
[7] K.-F. Chen *et al.*, Phys. Lett. B **725**, 378 (2013).
[8] Note that the ρ_{ui}, ρ_{iu} elements (i = 1–3) would easily generate large effects, hence would have to be rather small. This is consistent with the mass-mixing pattern.
[9] B. Altunkaynak *et al.*, Phys. Lett. B **751**, 135 (2015).
[10] See e.g. D. Chowdhury, O. Eberhardt, JHEP **1805**, 161 (2018); J. Haller *et al.*, Eur. Phys. J. C **78**, 675 (2018).
[11] G. Aad *et al.* [ATLAS and CMS Collaborations], JHEP **1608**, 045 (2016).
[12] W.-S. Hou, M. Kikuchi, EPL **123**, 11001 (2018).
[13] K. Fuyuto, W.-S. Hou, E. Senaha, Phys. Lett. B **776**, 402 (2018). This paper discusses further processes that are suppressed, or not, by $\cos\gamma$.
[14] M. Kohda, T. Modak, W.-S. Hou, Phys. Lett. B **776**, 379 (2018).
[15] For updates based on 13 TeV data, see M. Aaboud *et al.* [ATLAS Collaboration], JHEP **1710**, 129 (2017), and Phys. Rev. D **98**, 032002 (2018); A.M. Sirunyan *et al.* [CMS Collaboration], JHEP **1806**, 102 (2018).
[16] J. Brod, U. Haisch, J. Zupan, JHEP **1311**, 180 (2013).
[17] K. Nishiwaki, S. Niyogi, A. Shivaji, JHEP **1404**, 011 (2014).
[18] A. Djouadi, Phys. Rept. **459**, 1 (2008).
[19] J. Alwall *et al.*, JHEP **1407**, 079 (2014).
[20] R.D. Ball *et al.* [NNPDF Collaboration], Nucl. Phys. B **877**, 290 (2013).
[21] The Higgs Characterisation model `http://feynrules.irmp.ucl.ac.be/wiki/HiggsCharacterisation`
[22] A. Alloul *et al.*, Comput. Phys. Commun. **185**, 2250 (2014).
[23] F. Demartin *et al.*, Eur. Phys. J. C **74**, 3065 (2014).
[24] ATLAS Collaboration, ATL-PHYS-PUB-2014-016.
[25] CMS Collaboration, CMS-PAS-FTR-16-002.
[26] D. de Florian *et al.* [LHC Higgs Cross Section Working Group], arXiv:1610.07922 [hep-ph].
[27] While our two bands for $\mu_{t\bar{t}h}$ just illustrate the span from below to above 1 for final HL-LHC values, we note that $\mu_{t\bar{t}h}$ measurement itself would depend also on Γ_h.
[28] ATLAS Collaboration, ATL-PHYS-PUB-2015-024.
[29] J. Baron *et al.* [ACME Collaboration], Science **343**, 269 (2014).
[30] L. Evans, S. Michizono (Ed.) [Linear Collide Collaboration], arXiv:1711.00568 [physics.acc-ph].
[31] M.J. Boland *et al.* [CLIC and CLICdp Collaborations], arXiv:1608.07537 [physics.acc-ph].
[32] For beyond HL-LHC hadron collider physics, see e.g. the plenary talk by M.L. Mangano at Large Hadron Collider Physics conference, June 2018, Bologna, Italy.
[33] For a non-exhaustive list, see e.g. J. Ellis *et al.*, JHEP **1404**, 004 (2014); F. Boudjema *et al.*, Phys. Rev. D **92**, 015019 (2015); M.R. Buckley, D. Gonçalves, Phys. Rev. Lett. **116**, 091801 (2016); H.-L. Li *et al.*, Chin. Phys. C **40**, 063102 (2016); N. Mileo *et al.*, JHEP **1607**, 056 (2016); A.V. Gritsan *et al.*, Phys. Rev. D **94**, 055023 (2016); J. Li *et al.*, Phys. Lett. B **779**, 72 (2018); D. Gonçalves, K. Kong, J.H. Kim, JHEP **1806**, 079 (2018). and references therein.